

Magnetization reversal in nanostructured Co/Pd multilayers

Sug-Bong Choe and Sung-Chul Shin

Department of Physics, Korea Advanced Institute of Science and Technology, Taejon 305-701, Korea

(Received 17 April 1997; revised manuscript received 22 July 1997)

We report the experimental results on magnetization reversal in Co/Pd multilayers. Interestingly enough, reversal phenomena in this system were found to be strongly dependent on the magnetic properties varied with the Co-sublayer thickness. Direct domain observations and magnetization viscosity measurements revealed that wall motion was dominant in the samples having 2-Å-thick Co sublayer, whereas nucleation was dominant in those having 4-Å-thick Co sublayer. Magnetization reversal was theoretically studied using a nanomagnetic model and the strong dependence of reversal behavior on the magnetic properties could be qualitatively explained. [S0163-1829(98)02602-2]

I. INTRODUCTION

Co/Pd magnetic multilayers, which are artificially grown periodic layered structures of alternating Co and Pd materials, have been one of the most prospective candidates for the next generation of high-density magneto-optical recording media, due to their novel magnetic and magneto-optical properties.¹⁻⁴ Enormous studies have been carried out on the magnetic and magneto-optical properties of this system, but very little work has been done on the magnetization reversal mechanism.

Domain dynamics of magnetization reversal become very important in the high-density recording process, since it governs the formation of the written domain size, irregularity, and stability. Therefore, it is very important to understand the magnetization reversal mechanism for further improvement of recording performance as well as for the fundamental understanding of magnetism in thin films.

Previous observations of magnetization reversal in amorphous rare-earth transition-metal,⁵⁻⁷ sandwiched Co,⁸⁻¹⁰ Co-based alloys,¹¹ and multilayered systems¹²⁻¹⁵ have shown two limiting behaviors of magnetization reversal; wall-motion and nucleation dominant processes. The origin of these contrasting behaviors still remains controversial. Most of the experimental studies have explained that magnetization reversal behavior was mainly governed by structural properties such as local structural variation,⁶ film thickness,⁷ lattice mismatch,⁸ sublayer thickness,¹² and interfacial roughness.¹³ On the other hand, recent theoretical works based on two-dimensional micromagnetic simulation¹⁶⁻¹⁸ and the Ising system^{19,20} have reported that magnetization reversal behavior could be predicted with magnetic properties, without considering the detailed microstructure.

This paper is organized as follows: we present the experimental procedure in Sec. II, the experimental results and discussion on magnetization reversal in nanostructured Co/Pd multilayers in Sec. III, together with Monte Carlo simulation, and summarize our findings in Sec. IV.

II. EXPERIMENT

Co/Pd multilayers were prepared on glass substrates by e-beam evaporations of Co and Pd under the base pressure of 1.0×10^{-6} Torr. The multilayer structure was achieved by

alternatively exposing the substrate to two e-beam sources via a rotating substrate holder. Two sources of Co and Pd were physically separated by stainless-steel shields to prevent the cross contamination of their fluxes. The sources were screened with a shutter driven by a stepping motor in order to prevent deposition to the substrate during rotation of the substrate holder. The substrate holder was placed 25 cm above the sources. To achieve the intended sublayer thickness, the dwelling time of the substrate staying above each source was controlled by a computer interfaced to a stepping motor which drove the substrate holder. Typical deposition rates of 0.3 Å/s for Co and 0.5 Å/s for Pd, monitored by two corresponding quartz crystal sensors, were kept constant within a 10% fluctuation. The difference between the intended thickness and the actual thickness determined from low-angle x-ray diffraction turned out to be less than 2%. The samples had various Co-sublayer thicknesses of 2, 2.5, 3, 3.5, and 4 Å. But all samples had a constant Pd-sublayer thickness of 11 Å and the same number of repeats. Care was taken to maintain the same preparation conditions except the Co-sublayer thickness and the macroscopic magnetic properties were confirmed to be quite reproducible for the same nominal samples prepared in different runs.²¹ All samples in this study developed low-angle x-ray diffraction peaks, which suggested the existence of the multilayer structure in those samples.

Magnetization reversal behavior was studied by direct observation of domain structure using a magneto-optic microscope equipped with advanced video processing techniques as well as magnetization viscosity measurement monitoring the Kerr rotation angle at the wavelength of 6320 Å with time. In both experiments, the sample was first saturated by applying the magnetic field normal to the film plane and then, reversal behavior was investigated under reversing applied field smaller than the coercivity. Both experiments were taken under the same experimental condition, thus microscopic patterns of the reversing domain structure could be investigated along with the magnetization viscosity curves. The magnetization was measured using a highly sensitive vibrating sample magnetometer²² (VSM) calibrated against a Ni standard. The magnetic anisotropy was measured using a torque magnetometer at an applied field of 10 kOe. For both magnetization and anisotropy measurements, a small signal from the sample holder and uncoated substrate was sub-

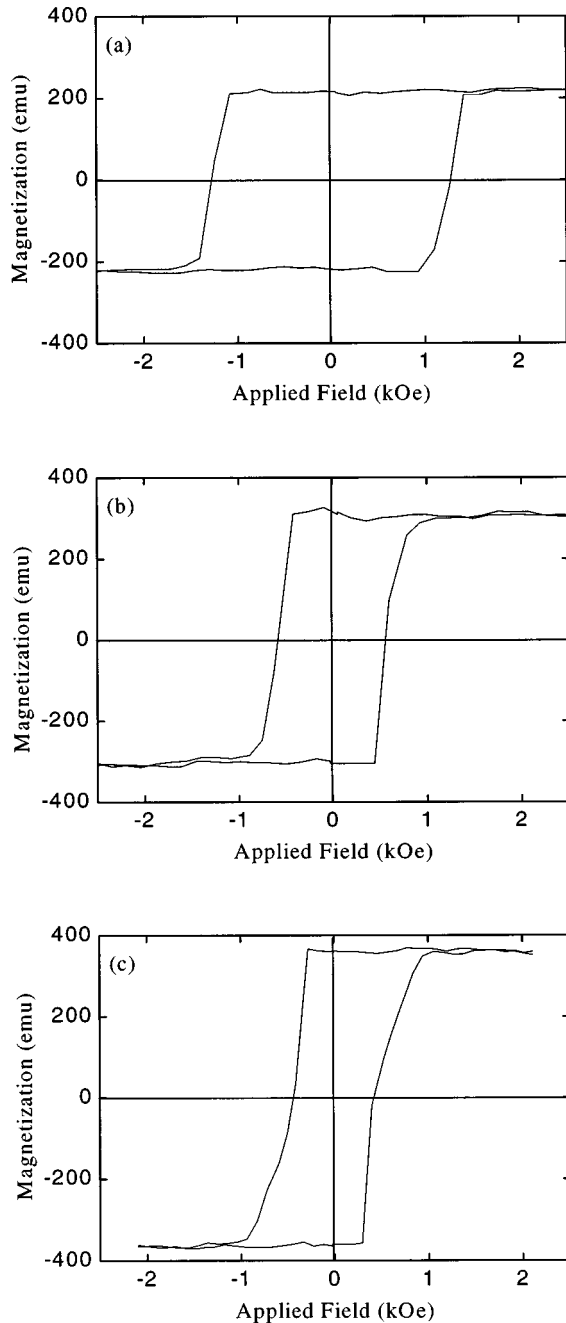


FIG. 1. Hysteresis loops measured by VSM for the samples of (a) 2, (b) 3, and (c) 4-Å-thick Co sublayers. Each sample has the saturation magnetization of 210, 300, and 370 emu/cc and the coercivity of 1.2, 0.6, and 0.4 kOe, respectively.

tracted out. We will designate the samples as $(t_{\text{Co}}\text{-}\text{\AA} \text{Co}/11\text{-}\text{\AA} \text{Pd})_n$, where t_{Co} is the Co-sublayer thickness and n is the number of repeats.

III. RESULTS AND DISCUSSION

All samples in this study had perpendicular magnetic anisotropy and showed the Kerr hysteresis loop of unit squareness. In Fig. 1, we exhibit the hysteresis loops measured by VSM for the samples of 2, 3, and 4-Å-thick Co sublayer. The $(2\text{-}\text{\AA} \text{Co}/11\text{-}\text{\AA} \text{Pd})_{10}$ multilayer exhibits a smaller magnitude of the saturation magnetization and a more square hysteresis

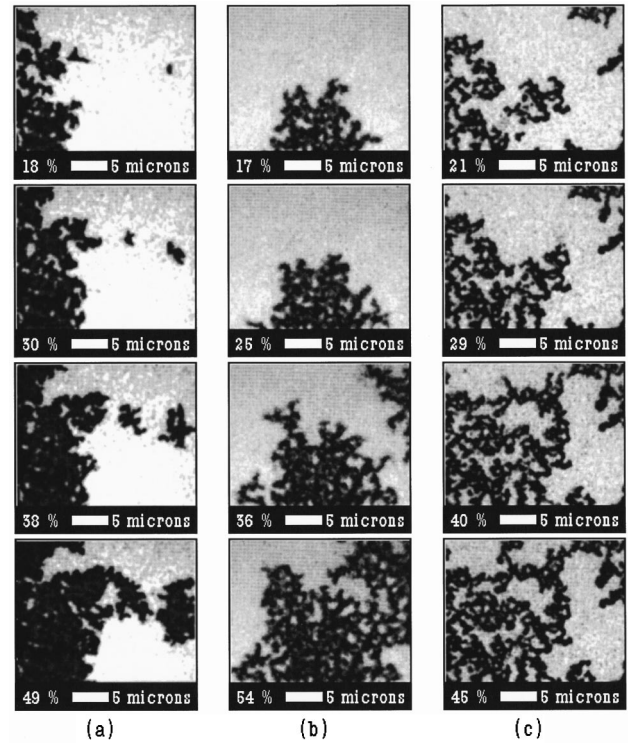


FIG. 2. Direct observation of the typical time-dependent domain patterns of (a) $(2\text{-}\text{\AA} \text{Co}/11\text{-}\text{\AA} \text{Pd})_{10}$ under $H=0.88 H_c$, (b) $(3\text{-}\text{\AA} \text{Co}/11\text{-}\text{\AA} \text{Pd})_{10}$ under $H=0.89 H_c$, and (c) $(4\text{-}\text{\AA} \text{Co}/11\text{-}\text{\AA} \text{Pd})_{10}$ under $H=0.83 H_c$. The percent denoted at the bottom of each frame is the areal fraction of the reversed domain.

loop than other samples. The slant hysteresis loop of the $(4\text{-}\text{\AA} \text{Co}/11\text{-}\text{\AA} \text{Pd})_{10}$ sample may be caused by a stronger strength of the demagnetizing field, because the magnetization reversal is more impeded for the sample having a larger demagnetizing field during the reversal process.¹⁸ The measured coercivities H_c are 1.2, 0.6, and 0.4 kOe for the samples of 2, 3, and 4-Å-thick Co-sublayer thickness, respectively.

Interestingly enough, reversal phenomena in this system were found to be very sensitively changed from wall-motion dominant reversal to a nucleation dominant one with increasing the Co-sublayer thickness from 2 to 4 Å. Gradual variation in domain reversal pattern was clearly observed even with a 0.5-Å increment in the Co-sublayer thickness. In Fig. 2, we show typical domain reversal patterns of $(2\text{-}\text{\AA} \text{Co}/11\text{-}\text{\AA} \text{Pd})_{10}$, $(3\text{-}\text{\AA} \text{Co}/11\text{-}\text{\AA} \text{Pd})_{10}$, and $(4\text{-}\text{\AA} \text{Co}/11\text{-}\text{\AA} \text{Pd})_{10}$ multilayers in order of increasing areal fractions of the reversed domains, taken under the applied fields smaller than the coercivities of the samples. Wall-motion dominant reversal in the $(2\text{-}\text{\AA} \text{Co}/11\text{-}\text{\AA} \text{Pd})_{10}$ sample can be vividly seen from Fig. 2(a). In this sample, a few nucleated domains were first formed in the beginning and gradually expanded in size at all domain boundaries by wall motion. Eventually, all domains of the sample were completely reversed. The domain evolution process was essentially the same irrespective of the magnitude of an applied field, but the rate of domain evolution was considerably accelerated by increasing the applied field. Even though the wall propagation speed was varied at different domain boundaries due to the wall pinning caused by local irregularities such as microstructural defects and interfacial roughness in the sample, magnetization reversal oc-

curred at all domain boundaries as seen in the figure. Thus, the microstructural irregularities are not the major factor in determining the reversal mechanism in this sample, but only yield the ragged wall boundaries.

In the $(4\text{-\AA Co}/11\text{-\AA Pd})_{10}$ sample, a magnetization reversal of dendritic growth is clearly observed as shown in Fig. 2(c). In this system, the once nucleated domain grew only slightly in size but expanded quickly by dendritic growth throughout the whole area of the sample. The dendritic stripes hardly grew in width, thus the widths of the stripes remained nearly constant during the reversal process. The unreversed region between the dendritic stripes remained unchanged even after a long time and could be reversed only by increasing an applied field close to the coercivity. More detailed investigation revealed that the dendritic stripes grew not by means of continuous expansion of the domain-wall boundary but by abrupt jutting-out of certain-sized sprouts adjacent to the existing domain boundary.⁵ The sizes of the sprouts were almost same during the whole reversal process and could be interpreted either as a cross-sectional area of the Barkhausen volume or a minimum size of nucleation.

In the $(3\text{-\AA Co}/11\text{-\AA Pd})_{10}$ sample, an intermediate reversal behavior of the samples mixed with domain-wall expansion and dendritic growth appeared as seen in Fig. 2(b). The magnetic domain reversed not only by the growth of random jutting-out stripes but also by the areal expansion of the domain wall in every domain boundary. Comparing with the complete reversal in Fig. 2(a), the unreversed areas surrounded by reversed areas still remained in Fig. 2(b). However, the fraction of the unreversed area is much smaller and the jutting-out domain size and the width of the stripe are much larger than the sample shown in Fig. 2(c).²³ Contrasting magnetization reversal behaviors dependent on the Co-sublayer thickness were again confirmed by magnetization viscosity measurements. In Fig. 3, we show the normalized time-dependent magnetization viscosity curves measured for the $(2\text{-\AA Co}/11\text{-\AA Pd})_{10}$, $(3\text{-\AA Co}/11\text{-\AA Pd})_{10}$, and $(4\text{-\AA Co}/11\text{-\AA Pd})_{10}$ samples under various reversed fields as denoted in the figures. The Kerr angle and time in the figure are normalized by a maximum Kerr angle and the half relaxation time, respectively. As mentioned earlier, the rate of relaxation is sensitively dependent on the strength of an applied field, but the basic shape of the normalized curves for a given sample remains the same irrespective of the applied field. However, the shapes of the curves among the samples are quite contrasting.

The $(2\text{-\AA Co}/11\text{-\AA Pd})_{10}$ multilayer shown in Fig. 3(a) exhibits initially a convex curve indicating a slow relaxation rate. Then, it shows more rapid relaxation with time and gradually approaches the complete reversal state. This shape of the curve is known to be a typical shape of thermally activated relaxation with rare nucleation probability and fast domain-wall motion. In this case, the initial relaxation rate is limited by the probability of nucleation, while the intermediate relaxation rate is governed by the successive domain-wall expansion.²⁴ The final equilibrium state is determined by the counterbalance of an applied field and the demagnetizing field, so that every curve reaches the saturation value due to the weak demagnetizing field in the $(2\text{-\AA Co}/11\text{-\AA Pd})_{10}$ sample. The magnetization viscosity curve is well matched with the observed domain reversal behaviors: few nucleation

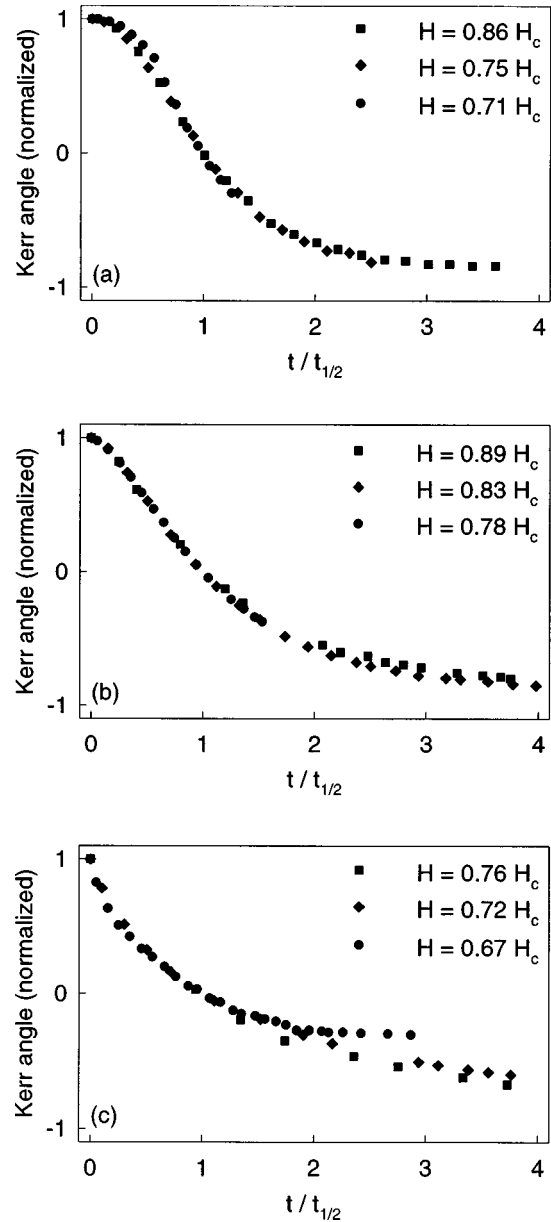


FIG. 3. Normalized viscosity curves under several reversing fields for (a) $(2\text{-\AA Co}/11\text{-\AA Pd})_{10}$, (b) $(3\text{-\AA Co}/11\text{-\AA Pd})_{10}$, and (c) $(4\text{-\AA Co}/11\text{-\AA Pd})_{10}$.

sites in the beginning and complete reversal via a wall-motion-dominant process.

In contrast, the $(4\text{-\AA Co}/11\text{-\AA Pd})_{10}$ multilayer in Fig. 3(c) exhibits initially a concave curve representing the fast decay rate and slowly approaches an equilibrium state. This shape of the curve can be interpreted as manifesting a typical behavior of thermally activated relaxation with large nucleation probability and slow domain-wall motion. It should be pointed out that due to a strong demagnetizing field in the $(4\text{-\AA Co}/11\text{-\AA Pd})_{10}$ sample, the degree of magnetization reversal is dependent on an applied field and complete reversal is never achieved at small applied fields even after a long time as seen in the figure. Though the viscosity measurement revealed the nucleation dominant reversal in the $(4\text{-\AA Co}/11\text{-\AA Pd})_{10}$ sample, the direct domain observation did not apparently show the truly nucleation dominant patterns but dendritic-growth ones. As mentioned above, the dendritic

growth was evolved by means of the abrupt jutting-out sprouts, which might be interpreted as a new upcoming nucleation adjacent to the existing domain boundary rather than as a domain-wall growth along the dendritic stripe patterns. The dendritelike domain patterns have been reported in many magnetic thin-film systems⁵ and more detailed investigations on the dendritelike growth are needed. The (3-Å Co/11-Å Pd)₁₀ sample in Fig. 3(b) shows nearly a linear dependence of magnetization relaxation in the beginning, which is a kind of intermediate shape between the convex and concave curves observed in Fig. 3(a) and Fig. 3(c), respectively. Thus, one might interpret this linear dependence as reflecting a thermally activated reversal behavior mixed with nucleation and wall-motion mechanisms.

To understand the observed reversal behaviors in Co/Pd multilayers, a theoretical study has been carried out by Monte Carlo simulation adopting a simple uniaxial anisotropy model, proposed by Kirby *et al.*¹⁶ In this model, the film is considered to be composed of nanosized identical single domain cells of volume V_c on hexagonal lattices lying in the XY plane with the periodic boundary condition.²⁵ Each cell has the saturation magnetization M_s , the uniaxial anisotropy K_u , and the exchange stiffness A_x . The magnetic energy E of a cell having magnetization angle θ from the $+z$ axis is given by

$$E = K_u V_c \sin^2 \theta - M_s V_c (H_z + H_d) \cos \theta + \left(3 - \frac{1}{2} \cos \theta \sum_k \cos \theta_k \right) E_w, \quad (1)$$

where the first term is the uniaxial anisotropy energy, the second term is the magnetostatic energy from the external field H_z normal to the film and the demagnetizing field H_d , and the last term is the domain-wall energy summed over the six boundaries to the nearest neighbors having the magnetization direction θ_k . The domain-wall energy E_w in one edge of a cell is calculated by the Bloch-wall approximation of the wall-energy density $4\sqrt{A_x K_u}$. The demagnetizing field H_d at the center of the cell is calculated by summing the magnetic field from the point dipoles at the center of other cells within the N th nearest cells. We took $N=20$ at which H_d was almost saturated to its asymptotic value.²⁶ The magnetic energy E has two minimums at $\theta=0$ and π with a maximum in between. The energy barrier to reverse is the difference in energy between the initial value and the maximum, and it is given by

$$E_B = K_u V_c \left[1 + \cos \theta \frac{M_s V_c (H_z + H_d) + \frac{1}{2} E_w \sum_k \cos \theta_k}{2 K_u V_c} \right]^2, \quad (2)$$

where θ and θ_k are the initial magnetization direction of the cell and the nearest neighbors, respectively. The probability P of a cell to reverse through the energy barrier E_B by thermally activated fluctuation in time Δt is

$$P = P_0 \exp(-E_B/k_B T) \Delta t, \quad (3)$$

where P_0 is the probability constant, k_B is Boltzmann's constant, and T is the temperature. The value $P_0 \Delta t$ is deter-

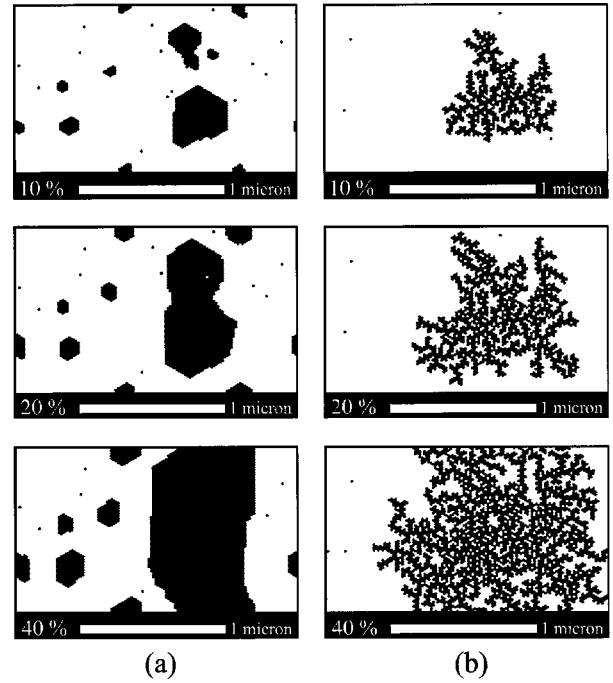


FIG. 4. Simulated patterns of domain development. (a) (2-Å Co/11-Å Pd)₁₀ with $M_s=210$ emu/cc, $K_u=4.5 \times 10^6$ erg/cc, and $A_x=3.5 \times 10^{-7}$ erg/cm, and (b) (4-Å Co/11-Å Pd)₁₀ with $M_s=370$ emu/cc, $K_u=4.5 \times 10^6$ erg/cc, and $A_x=6.2 \times 10^{-7}$ erg/cm. All figures were obtained under $H=0.99 H'_c$, where H'_c was determined by the equation of $H'_c=2K_u/M_s-4\pi M_s$. The percent denoted at the bottom of each frame is the areal fraction of the reversed domain. We assumed Bloch wall transition configuration.

mined to make the maximum P equal to $1/N$ by preliminary calculating $P/P_0 \Delta t$ over the whole sample. A cell is determined to be reversed when a random value ranging $[0,1]$ is greater than the probability P of the cell and then, the total domain pattern is constructed from each state of the individual cell calculated by the checkerboard scanning method.²⁶ Magnetization reversal of Co/Pd multilayers has been investigated by the above simulation of 64×128 cells. In the simulation, V_c was taken as 2.92×10^{-18} cc and no detailed microstructure was considered. Thus, the reversal probability of each cell is expressed mainly by the macroscopic magnetic parameters. The values of M_s and K_u used in the simulation were experimentally determined, whereas a reported bulk value was used to determine A_x of each multilayered structure of the samples.²⁷ We assumed that the in-plane exchange interaction lied only in the Co sublayer, not in the Pd sublayer and thus, the effective A_x of the multilayer was considered to be increased with increasing the Co-sublayer thickness. The values of M_s and A_x were substantially increased with the Co-sublayer thickness, but the change in K_u among the samples was not noticeable because the ratio between the surface-induced anisotropy and the Pd-sublayer thickness in our multilayered system was almost the same as the crystalline anisotropy of the Co sublayer.

In Fig. 4, we present simulated domain-reversal patterns for (2-Å Co/11-Å Pd)₁₀ and (4-Å Co/11-Å Pd)₁₀ multilayers with respect to the areal fraction of the reversed domain. It is very interesting to note that the shapes of the simulated domain reversal patterns with the Co-sublayer thickness are basically the same as those of the experimental ones. Con-

sidering the fact that the theoretical prediction was obtained by assuming identical cells of uniform films with the macroscopic magnetic values, good correspondence between the experimental observation and the theoretical prediction implies an essential role of the macroscopic magnetic properties on the domain reversal mechanism. The reversal mechanism is determined by the competition between a new upcoming nucleation probability and the gradual wall-expansion probability, where both probabilities are governed via thermally activated process determined by the macroscopic magnetic properties.¹⁸ These reversal behaviors are quite understandable by considering the domain configuration of the ground energy state. The multilayer of the thinner Co sublayer has weak demagnetization energy due to its weak magnetization and thus, it prefers large domain configuration to reduce the domain boundary length due to the relatively strong domain-wall energy. The large domain should be achieved by the wall-motion process from the typical-sized nucleation center and thus, the multilayer shows the wall-motion dominant reversal behavior. On the other hand, the multilayer of the thicker Co sublayer has strong demagnetization energy and thus, the domain splits into the narrow stripe patterns to minimize the demagnetization energy. Therefore, in this multilayer it is quite natural to observe the dendritic stripe growth from the nucleation center by the thermally activated relaxation to the stripe domain configuration of the ground energy state.

It has been reported that the reversal mechanism was greatly influenced by large structural variation caused by very different preparation conditions.^{6,7,13} However, the microstructural effect on the reversal mechanism in our sample is believed to be negligible, because the samples were fabricated in the same preparation conditions with the total thickness of 130–150 nm. Atomic-sized irregularities due to the

lattice mismatching and the residual stress were also suggested and examined as a possible origin of the contrasting reversal behaviors.^{8,12,14} However, such small-sized irregularities are expected to interact with the domain-wall propagation not by individual interaction but by cumulative interaction of overall irregularities, due to much larger domain sizes than structural irregularities. For the domain dynamics, the effects of atomic-sized irregularities should be treated as an averaged property over the size of the domain wall and therefore, the domain wall cannot feel any local structural variation of atomic-sized irregularities.

IV. CONCLUSIONS

We have investigated magnetization reversal of Co/Pd multilayers by direct observations of domain patterns and time-dependent measurements of the magnetization viscosity curves. We have demonstrated that the magnetization reversal phenomena in this system were sensitively changed from wall-motion dominant reversal to a dendritic-growth dominant one with ranging the Co-sublayer thickness from 2 to 4 Å. The dendritic-growth pattern is believed to be a kind of microscopic domain pattern caused by the nucleation dominant reversal mechanism. Based on a nanomagnetic computer simulation without considering detailed microstructural properties, we conclude that the domain reversal behavior in this system is mainly governed by the macroscopic magnetic properties.

ACKNOWLEDGMENTS

This work was supported by Korea Science and Engineering Foundation (KOSEF) and the Ministry of Science and Technology of Korea.

-
- ¹P. F. Carcia, A. D. Meinhaldt, and A. Suna, *Appl. Phys. Lett.* **47**, 178 (1985).
- ²S. Hashimoto, Y. Ochiai, and K. Aso, *J. Appl. Phys.* **66**, 4909 (1989).
- ³H. J. G. Draaisma, W. J. M. de Jonge, and F. J. A. den Broeder, *J. Magn. Magn. Mater.* **66**, 351 (1987).
- ⁴S.-C. Shin, J.-H. Kim, and D.-H. Ahn, *J. Appl. Phys.* **69**, 5664 (1991).
- ⁵C.-J. Lin, J. C. Suit, and R. H. Geiss, *J. Appl. Phys.* **63**, 3835 (1988).
- ⁶H.-P. D. Shieh and M. H. Kryder, *IEEE Trans. Magn.* **MAG-24**, 2464 (1988).
- ⁷T. G. Pokhil and N. Nikolaev, *IEEE Trans. Magn.* **MAG-29**, 2536 (1993).
- ⁸J. Pommier, P. Meyer, G. Pénissard, J. Ferré, P. Bruno, and D. Renard, *Phys. Rev. Lett.* **65**, 2054 (1990).
- ⁹G. Bayreuther, P. Bruno, G. Lugert, and C. Turtur, *Phys. Rev. B* **40**, 7399 (1989).
- ¹⁰A. Kirilyuk, J. Ferré, J. Pommier, and D. Renard, *J. Magn. Magn. Mater.* **121**, 536 (1993).
- ¹¹T. Kleinfeld, J. Valentin, and D. Weller, *J. Magn. Magn. Mater.* **148**, 249 (1995).
- ¹²R. D. Kirby, J. X. Shen, Z. S. Shan, and D. J. Sellmyer, *J. Appl. Phys.* **70**, 6200 (1991).
- ¹³J. X. Shen, R. D. Kirby, Z. S. Shan, D. J. Sellmyer, and T. Suzuki, *J. Appl. Phys.* **73**, 6418 (1993).
- ¹⁴Z. S. Shan, J. X. Shen, R. D. Kirby, D. J. Sellmyer, and Y. J. Wang, *J. Appl. Phys.* **75**, 6418 (1994).
- ¹⁵S.-B. Choe and S.-C. Shin, *J. Appl. Phys.* **81**, 5743 (1997).
- ¹⁶R. D. Kirby, J. X. Shen, R. J. Hardy, and D. J. Sellmyer, *Phys. Rev. B* **49**, 10 810 (1994).
- ¹⁷U. Nowak, *IEEE Trans. Magn.* **MAG-31**, 4169 (1995).
- ¹⁸A. Lyberatos, J. Earl, and R. W. Chantrell, *Phys. Rev. B* **53**, 5493 (1996).
- ¹⁹H. L. Richards, M. A. Novotny, and P. A. Rikvold, *Phys. Rev. B* **54**, 4113 (1996).
- ²⁰L. C. Sampaio, M. P. de Albuquerque, and F. S. de Menezes, *Phys. Rev. B* **54**, 6465 (1996).
- ²¹S.-B. Choe and S.-C. Shin, *Korean Appl. Phys.* **9**, 674 (1996).
- ²²M.-G. Kim and S.-C. Shin, *Korean Appl. Phys.* **9**, 575 (1996).
- ²³D. M. Donnet, V. G. Lewis, J. N. Chapman, K. O'Grady, and H. W. van Kesteren, *J. Phys. D* **26**, 1741 (1993).
- ²⁴M. Labrune, S. Andrieu, F. Rio, and P. Bernstein, *J. Magn. Magn. Mater.* **80**, 211 (1989).
- ²⁵M. Mansuripur, *J. Appl. Phys.* **66**, 3731 (1989).
- ²⁶M. Mansuripur, *J. Appl. Phys.* **61**, 1580 (1987).
- ²⁷S.-C. Shin, *Appl. Surf. Sci.* **65**, 110 (1993).